CHIRAL SYMMETRY IN MATTER*

R.A. JANIK[a], M.A. NOWAK[a,b], G. PAPP[c] AND I. ZAHED[d]

[a] Department of Physics, Jagellonian University, 30-059 Krakow, Poland.
[b] GSI, Plankstr. 1, D-64291 Darmstadt, Germany &
Institut für Kernphysik, TH Darmstadt, D-64289 Darmstadt, Germany
[c] GSI, Plankstr. 1, D-64291 Darmstadt, Germany &
Institute for Theoretical Physics, Eötvös University, Budapest, Hungary
[d] Department of Physics, SUNY, Stony Brook, New York 11794, USA

(Received October 9, 1996)

We provide a schematic view to some general aspects of chiral symmetry in matter using mean-field arguments. We use a simplified version of the Nambu–Jona–Lasinio model to formulate the ideas behind the thermodynamics at work in a variety of models with spontaneously broken chiral symmetry but without confinement. This version of the model is mapped onto chiral random matrix models, with some emphasis on the bulk behavior of the corresponding Dirac spectrum. Phase changes in the simplified model show up in the form of a rearrangement in the Dirac spectrum, with edge singularities that follow from mean-field exponents. The results are shared by a variety of models, and seem to be in quantitative agreement with some QCD lattice simulations. We comment on the relevance of microscopic and macroscopic universality in random matrix models, and the possible motivation for these models from QCD.

PACS numbers: 11.30.-j, 12.38.-t, 12.38.Aw, 12.90.+b

1. Introduction

Chiral symmetry is one of the most fundamental properties of strong interactions. Major experiments in the near future will hopefully help clarify this issue — HADES (GSI), RHIC (BNL), LHC (CERN). Several encouraging results are available even now — experiments like CERES and HELIOS3 are suggesting that finite density/temperature effects applied to the vacuum state of QCD do seem to change the composition of hadrons [1]. Despite these exciting experimental endeavors, an explanation for why chiral symmetry is spontaneously broken in the QCD vacuum from first principles is

* Presented at the "Meson 96" Workshop, Cracow, Poland, May 10–14, 1996.

still not unanimous. A number of tools and ideas have been devised to try to understand this issue and assess its phenomenological implications : Lattice calculations [2], variational models (*e.g.* instantons [3]), sum rules [4], chiral perturbation theory [5], Nambu–Jona–Lasinio (NJL) models [6], Walecka models [7], random matrix models [8], to mention a few [9].

In this lecture we will expose a certain point of view where the mean-field description plays a prominent role in the discussion of a variety of questions. While not unanimous, this description captures the essentials of a variety of **models** (NJL models, instanton models, random matrix models) with their inherent advantages and disadvantages. It is fair to say, that this point of view has been the motto of Gerry Brown for many years. This paper is a small tribute to his seventieth birthday.

In Section 2 we formulate a schematic version of the NJL model, focusing on the constituent quark spectrum and its ensuing thermodynamics, ignoring the issue of confinement. In Section 3 we review the Banks–Casher formula and suggest that the quark spectrum may be important in addressing the issue of spontaneous chiral symmetry breaking both in vacuum and matter. In Section 4, we map the schematic version of the NJL model onto chiral random matrix models. The general lore of determinism versus chance in the infrared is discussed. In Section 5, a generic classification of the Dirac spectra is proposed in the mean-field approximation using algebraic equations. In Section 6, some of these ideas are applied to the Columbia lattice data at finite temperature. In Section 7, we show that the mean-field analysis at finite density is upset by fluctuations, exposing some difficulties both in the models and in the lattice simulations. In Section 8, we put forward some speculative arguments on the relationship between chiral random matrix models and fundamental QCD. In Section 9 we discuss the relevance of microscopic and macroscopic universality in random matrix models. Our conclusions and recommendations are given in Section 10.

2. Two-level NJL model

Consider a single flavor version of the NJL model in four dimensional Euclidean space [9, 10],

$$\mathcal{L}_4 = \psi^\dagger(i\gamma\cdot\partial + im + i\mu\gamma_4)\psi + \frac{g^2}{2}\Big((\psi^\dagger\psi)^2 + (\psi^\dagger i\gamma_5\psi)^2\Big) \tag{1}$$

or equivalently

$$\begin{aligned}\mathcal{L}_4 \;=\; & +\psi_R^\dagger(i\gamma\cdot\partial + i\mu\gamma_4)\psi_L + \psi_L^\dagger(i\gamma\cdot\partial + i\mu\gamma_4)\psi_R \\ & +\psi_R^\dagger\, i(P+m)\,\psi_R + \psi_L^\dagger i(P^\dagger+m)\psi_L + \frac{1}{2g^2}PP^\dagger\end{aligned} \tag{2}$$

in the chiral quark basis $\psi = (\psi_R, \psi_L)$ with the right and left projectors $(1 \pm \gamma_5)/2$. Here P, $P^\dagger$ stand for independent auxiliary fields, g is a fixed coupling and μ is a real chemical potential. Note that the Minkowski fields follow from the Euclidean fields through $(i\psi^\dagger, \psi) \to (\overline{\psi}, \psi)$. In particular, $m\psi^\dagger\psi$ is the mass term in Euclidean space compared to $m\bar{\psi}\psi$ in Minkowski space. This form of the mass term is enforced by the fact that the Lorentz group is SO(4) in Euclidean space and SO(3,1) in Minkowski space. This means that the chirality breaking terms in Euclidean space are rather $L^\dagger L$ and $R^\dagger R$ than $R^\dagger L$ and $L^\dagger R$ as in Minkowski space. With these conventions, the kinetic term in Minkowski space preserves chirality but flips it in Euclidean space. Equation (2) is defined on the strip $\beta \times V_3$ in Euclidean space, with $P(\tau + \beta, \boldsymbol{x}) = P(\tau, \boldsymbol{x})$, and $\psi(\tau + \beta, \boldsymbol{x}) = -\psi(\tau, \boldsymbol{x})$.

For our purposes, further simplifications are needed. The anti-periodicity of the quark fields yields

$$\psi(\tau, \boldsymbol{x}) = \sum_{n=-\infty}^{+\infty} \mathrm{e}^{-i\omega_n \tau}\, \psi_n^{\boldsymbol{x}}\,, \tag{3}$$

where $\omega_n = (2n+1)\pi T$ are the Matsubara frequencies ($T = 1/\beta$), and $\boldsymbol{x} = 1, 2, \ldots, N$ label discrete points in three dimensional space. Space is here a grid of dimension N, where each point contains quarks of frequency ω_n and chirality L (left-handed) and R (right-handed). If we further assume that the auxiliary fields P, $P^\dagger$ are constant in space and time, the action in (2) reduces dimensionally to a 0-dimensional one with infinitely many Matsubara modes. The corresponding partition function can be readily found in the form

$$Z[T, \mu] = \int dP\, dP^\dagger\, \mathrm{e}^{-N\beta\Sigma PP^\dagger} \prod_{n=-\infty}^{+\infty} \det{}_2^N \beta \begin{pmatrix} i(m+P) & \omega_n + i\mu \\ \omega_n + i\mu & i(m+P^\dagger) \end{pmatrix} \tag{4}$$

following the rescaling $q_n^{\boldsymbol{x}} = \sqrt{V_3}\psi_n^{\boldsymbol{x}}$ and $\Sigma = V_3/2g^2$, where $q_n^{\boldsymbol{x}}$ are now dimensionless Grassmann (anticommuting) variables. The determinant in (4) is over 2×2 matrices. For completeness we observe that (4) corresponds also to the 0-dimensional Lagrangian density

$$\mathcal{L}_0 = q^\dagger((\boldsymbol{\Omega} + i\mu)\gamma_4 + im)q + \frac{1}{N\Sigma}(q_R^\dagger q_R)\,(q_L^\dagger q_L) \tag{5}$$

with $\boldsymbol{\Omega} = \omega_n \mathbf{1}_n \otimes \mathbf{1}_x$. We note that a constant P implies that only certain combinations of the Matsubara modes are allowed to interact with each other. Other choices are also possible. At high temperature, all ensembles become the same since they are dominated by the two lowest Matsubara modes $\omega_0 = +\pi T$ and $\omega_{-1} = -\pi T$ (see below).

To discuss the thermodynamics of the above model, it is more intuitive to use (4) in large N with $\boldsymbol{n} = N/V_3$ fixed. The effective potential associated to (4) reads

$$H = N\Sigma PP^\dagger - NT \sum_{n=-\infty}^{+\infty} \ln\beta^2 \left(\omega^2 + (\omega_n + i\mu)^2\right) , \tag{6}$$

where

$$\omega = \sqrt{(P+m)(P^\dagger+m)} . \tag{7}$$

The sum in (6) can be done using standard methods [11], and the answer is

$$H = N\Sigma PP^\dagger - N\left(\omega + T\ln\prod_{\pm}(1+\mathrm{e}^{-(\omega\mp\mu)/T})\right) . \tag{8}$$

The first term is a simple version of the vacuum energy, while the second term combines the contribution from the "Dirac sea" and matter. In this schematic model, the Dirac spectrum is simplified to two-levels in frequency space ($\pm\omega$) for each $\boldsymbol{x} = 1, 2, \ldots, N$, and for each handedness L, R. Recall that $N_F = 1$. This model will be referred to as a two-level NJL model. There is no kinetic energy associated to the quarks in (4). The pressure at high temperature reads

$$\boldsymbol{P} = T\frac{\partial \ln Z}{\partial V_3} = 2\boldsymbol{n}T\ln 2 - \boldsymbol{n}\Sigma PP^\dagger + \mathcal{O}(\frac{1}{T}) . \tag{9}$$

The first term is the thermal pressure of free constituent quarks, while the second term is a vacuum energy. At these temperatures, the pion contribution is **dwarfed** by the constituent quark contribution ($1 : N$), a point that is largely due to the lack of confinement. Does it make sense at all? In a way, if we were to think about (9) as a way to describe a chiral phase transition from the high temperature side. Clearly (9) is inappropriate for discussing the low temperature phase of confining theories. In large N, the extremum of the effective potential (8) yields a gap equation for P_* (we restrict here the solutions to the case $P = P^\dagger$)

$$2P_*\Sigma = 1 - n - \overline{n} , \tag{10}$$

where $n = (\mathrm{e}^{(\omega_*-\mu)/T}+1)^{-1}$ for particles and $\overline{n} = (\mathrm{e}^{(\omega_*+\mu)/T}+1)^{-1}$ for antiparticles. The constituent quark density is

$$\rho_Q = i\langle\psi^\dagger\gamma_4\psi\rangle = \frac{T}{V_3}\frac{\partial \ln Z}{\partial\mu} = -\frac{T}{V_3}\frac{\partial H}{\partial\mu} = \boldsymbol{n}\,(n - \overline{n}) , \tag{11}$$

while the quark condensate is

$$i\langle\psi^\dagger\psi\rangle = \frac{1}{V_3}\frac{\partial \ln Z}{\partial m} = \frac{1}{V_3}\frac{\partial H}{\partial m} = -2n\,\Sigma P_* \,. \tag{12}$$

A non-vanishing P implies a non-vanishing quark condensate, hence a spontaneous breaking of chiral symmetry. The relations (10-12) are just schematic versions of the usual gap, density and condensate relations in the NJL models [6].

For zero current mass m, the gap equation (10) admits solutions only for $T \leq T_c = 1/(4\Sigma)$. For non-zero current mass m there is always a solution, *albeit* with $P \sim m$ for $T \sim T_c$ and $m \sim 0$. At high temperature *and* for $T \approx T_c$ the gap equation (10) simplifies to

$$g(P_* + m)^3 + \mu^2(P_* + m) - h = \mathcal{O}\left(\frac{1}{T}\right) \tag{13}$$

with $h = m$, $\mu^2 = (T - T_c)/T_c$ and $g = (12T_c^2)^{-1}$. Eq. (13) has the generic form of a cubic equation, as expected from mean-field treatments of chiral phase transitions [12]. Indeed, (13) is just the gap equation generated from the effective potential [12]

$$\mathcal{L}_0(T,\phi) = -h\Phi + \tfrac{1}{2}\mu^2\Phi^2 - \frac{c}{N_F}\Phi^{N_F} + \frac{g}{4}\Phi^4 \,, \tag{14}$$

where in the present case $c = 0$.

The high temperature expansion through (13) provides an accurate description of the chiral phase transition in our model (4) that is consistent with mean-field universality. Indeed, from (13) it follows that at $T = T_c$, and for a weak external field h (current mass), $P \sim h^{1/3}$, and hence the critical exponent $\delta = 3$. For $h = 0$ but $T \neq T_c$, $P \sim (T - T_c)^{1/2}$. Since the chiral condensate $i\langle\psi^\dagger\psi\rangle \sim P$, the next critical exponent $\beta = 1/2$. Moreover, from (9) the pressure $\boldsymbol{P} \sim T$, so that the specific heat $C \sim (T - T_c)^0$ with a critical exponent $\alpha = 0$. The scalar quark susceptibility

$$\chi(T) = \langle\left(\psi^\dagger\psi - \langle\psi^\dagger\psi\rangle\right)^2\rangle \,, \tag{15}$$

measures the correlation length produced by the exchange of a constant scalar in the model. It is saturated by the scalar mass, $\chi \sim 1/m_\sigma^2$. The latter follows from (4) by shifting $P = P_* + \sigma$ around the saddle point solution. In the Gaussian approximation $m_\sigma = 2P_*$. Thus $\chi \sim (T - T_c)^{-1}$ with a critical exponent $\gamma = 1$. Finally, since the model considered does not have any space-time dependence, it is not possible to use it to analyze the ν and η critical exponents. It is however straightforward to understand that in

the NJL model, we expect that in the pion-channel π with $P = P_* + \sigma + i\pi$, the asymptotics is

$$C_\pi(x,T) \sim \frac{1}{|\vec{x}|}\, \mathrm{e}^{-m_\pi(T)\,|\vec{x}|}\,. \tag{16}$$

Thus the spatial correlation length at T_c is

$$\xi \sim \frac{1}{m_\pi(T)} \sim \frac{1}{i\langle\psi^\dagger\psi\rangle} \sim (T - T_c)^{-1/2} \tag{17}$$

with critical exponents $\nu = 1/2$ and $\eta = 0$. The set of all critical exponents derived so far $(\alpha, \beta, \gamma, \delta, \nu, \eta) = (0, 1/2, 1, 3, 1/2, 0)$ is known as the set of mean-field exponents. They are universal and characterize a phase transition that is second-order and of the type discussed by Landau and Ginzburg.

The role of the chemical potential in the present description can be best seen by specializing to $T = 0$. In this case, $n = \Theta(\mu - \omega)$ and $\overline{n} = 0$, where Θ is a step function. Clearly, $\rho_Q \neq 0$ only when the chemical potential $\mu \geq \omega$, in which case $P = 0$ and hence a vanishing quark condensate. The space independent quark modes have a Fermi surface that is sitting precisely at the level $+\omega$. Any finite quark density causes a restoration of chiral symmetry, since the latter is caused by the asymmetry in the spectrum obtained by populating the mode $-\omega$. To achieve more one has to take into account the space-variation of the quark wave-function, which leads to a field-theory rather than a matrix model. In this case, we are back to the NJL descriptions or QCD itself. The situation $0 \leq \mu \leq \omega$ does not support any finite density (Fermi-level in the Dirac gap). Since ω plays in our case, the role of a (shifted) constituent mass, chiral symmetry is restored for $\mu \sim \omega \sim m_N/3$, where the nucleon mass m_N is qualitatively set equal to three times the constituent quark mass ω. From our discussion, the transition is sharply first order and occurs at zero baryon density.

To summarize: in the two-level version of the NJL model described here, the **naive** low-lying spectrum is composed of constituent quarks and mesons. In the ground state, the quark-antiquark interaction is attractive in the singlet-isosinglet channel, providing a simple mechanism for the spontaneous breakdown of chiral symmetry, through the condensation of quarks. With increasing density or temperature, the constituent quarks in the heat bath (temperature) or Fermi level (density) overcome the "asymmetry" produced by the quarks in the Dirac sea, thereby restoring chiral symmetry at a critical temperature or density. The transition is mean-field in nature, and mostly driven by entropy. In so far, we have kept silent about the thermodynamical relevance of the multiquark states since the model lacks confinement. This point will be discussed below.

3. Banks-Casher relation and the Dirac spectrum

Since chiral symmetry is a property of the quark wave-functions, to what extent a chiral phase transition reflects itself on the quark spectrum? Important insights to this question can be gained by recalling the basic relation derived by Banks and Casher [13]. In four Euclidean space dimensions, the quark propagator in a fixed gluon background A reads

$$S(x,y,A) = \langle 0|q(x)\bar{q}(y)|0\rangle = \langle 0|(-i\not{D}(A) - im)^{-1}|0\rangle. \tag{18}$$

The spectral representation for the propagator gives

$$S(x,y,A) = \sum_n \frac{\phi_n(x)\phi_n^\dagger(y)}{-\lambda_n - im}, \tag{19}$$

where ϕ_n, λ_n are eigenvectors and eigenvalues of the Dirac equation

$$i\not{D}(A)\phi_n(x) = \lambda_n\phi_n(x). \tag{20}$$

Thus the fermion condensate in Euclidean space is

$$\langle q^\dagger q\rangle = -\lim_{x\to y}\langle q(x)q^\dagger(y)\rangle_A = -\langle \operatorname{Tr} S(x,x,A)\rangle_A, \tag{21}$$

where $\langle\ldots\rangle_A$ denotes the averaging over all the gluonic configurations A using the QCD action. In the limit where the four-volume V_4 goes to infinity, the spectrum becomes dense and we may replace the sum over the states by an integration over the mean spectral density

$$\nu(\lambda) = \left\langle \sum_n \delta(\lambda - \lambda_n)\right\rangle_A. \tag{22}$$

In terms of (22) the fermion condensate (21) becomes

$$\langle q^\dagger q\rangle = -\langle \operatorname{Tr}(-i\not{D}(A) - im)^{-1}\rangle_A = \frac{1}{V_4}\int d\lambda \frac{\nu(\lambda)}{\lambda + im}. \tag{23}$$

In the chiral limit, $m \to 0$, the Dirac operator $\not{D}$ anticommutes with γ_5, so the non-zero eigenvalues come in pairs $(\lambda, -\lambda)$ and the spectral function is symmetric. Inserting

$$\lim_{m\to 0+}\frac{1}{\lambda \pm im} = \mathrm{P}\frac{1}{\lambda} \mp i\pi\delta(\lambda) \tag{24}$$

into (23) and using the fact that the principle-value part drops out for even-spectra, we obtain

$$\langle q^\dagger q \rangle = -\frac{i\pi}{V_4}\nu(0)\,. \tag{25}$$

A Wick rotation to Minkowski space $(q^\dagger, q) \to (i\bar{q}, q)$ gives[1] [13]

$$\langle \bar{q}q \rangle = -\frac{\pi}{V_4}\nu(0)\,. \tag{26}$$

This relation states that for chiral symmetry to be broken in four dimensions, the number of quark eigenmodes near zero virtuality has to grow like V_4 in contrast to $\sqrt[4]{V_4}$ in free space. For this argument to hold, it is very important that the chiral limit $m \to 0$ is taken after the thermodynamical limit $V_4 \to \infty$, for otherwise the result would be zero. The spontaneous breakdown of a continuous symmetry cannot take place in finite volumes, unless the condition $m\langle \bar{q}q \rangle V_4 \ll 1$ is fulfilled.

Various possibilities for the Dirac spectrum near zero virtuality can be entertained in light of (26). Three typical behaviors are shown in Fig. 1. Fig. 1a exhibits a bounded mean eigenvalue distribution with a number at zero virtuality that is of the order of V_4, thus a non-vanishing quark condensate. This is typical of a ground state with a spontaneously broken chiral symmetry. Fig. 1b shows a bounded spectrum with a dip at zero virtuality, that is wider than $1/V_4$, thus a vanishing quark condensate. This is typical of a state with unbroken chiral symmetry. Fig. 1c shows an unbounded but typical spectrum for the QCD ground state. The dip at the origin is caused by Airy oscillations (quenched) and fermionic level-repulsion (unquenched), and disappears in the thermodynamical limit.

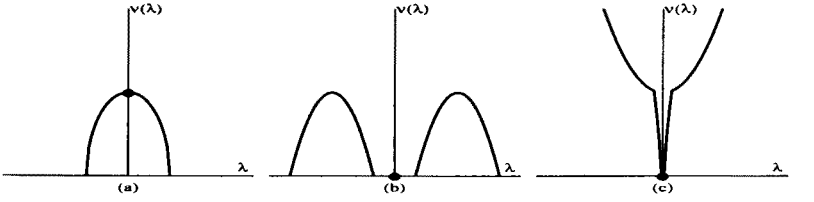

Fig. 1. Typical Dirac spectra.

What causes the mean spectral density $\nu(\lambda)$ to be non-vanishing at zero virtuality? In their seminal paper, Banks and Casher [13] have argued that in the first quantized version of QCD, the quarks in four dimensions undergo

[1] We note that the quark condensate is complex in Euclidean space and real in Minkowski space.

random walks scattering on the gauge fields, that should turn quasi-one-dimensional because of confinement. A convincing case was made in strong coupling and quenched lattice QCD. In what follows, we will entertain an alternative suggestion in the second quantized version of phenomenologically inspired models (instanton models, NJL models), in which the quark states undergo delocalization near zero virtuality. This idea was originally due to Casher and Neuberger [14]. A quantitative assessment of this idea can only be made if we were to further **assume** that in the Dirac spectrum typical of QCD (see for instance Fig. 1c above), there is a scale separation between the soft and hard modes, all the way to the transition point, that is

$$\nu(\lambda) \approx \nu_H(\lambda) + \nu_S(\lambda) \tag{27}$$

with typically $\nu_H(\lambda) \sim N_c|\lambda|^3/4\pi^2$ in the chiral limit, and $\nu_S(\lambda)$ a bounded function. Wilson lattice spectra simulations by Kalkreuter [15] suggest such a possibility, although the cubic growth from the hard modes is not really visible, given the character of the quark dispersion relation on the lattice. A clear test of this assumption would be to repeat the same calculations with cooled lattice configurations. The separation (27) would be assumed throughout even at the transition point, and the analysis will be carried out for the soft part $\nu_S(\lambda)$ or $\nu(\lambda)$ for short.

4. Two-level NJL model: randomness vs determinism

The relation between the quark condensate and the Dirac spectrum as unraveled by (26) can be discussed in the context of the two-level NJL model by rewriting the model in random bosonic variables. For that, consider the new auxiliary matrix $\boldsymbol{A}^{\boldsymbol{x},\boldsymbol{y}}_{n,m}$ with entries both in ordinary space $\boldsymbol{x}, \boldsymbol{y}$ and frequency space n, m. $\boldsymbol{A}$ is a doubly banded, complex matrix with dimensions $(N \times N) \otimes (\infty \times \infty)$. In contrast with P, the matrix $\boldsymbol{A}$ bosonizes pairs of quarks of opposite chirality. For the lowest two Matsubara frequencies it is simply $(N \times N) \otimes (2 \times 2)$ matrix . In terms of $\boldsymbol{A}$, Eq. (5) becomes

$$\mathcal{L}_0 = +q^\dagger((\boldsymbol{\Omega} + i\mu)\gamma_4 + im)q + N\Sigma \mathrm{Tr}_{\boldsymbol{x},n}(\boldsymbol{A}\boldsymbol{A}^\dagger) + q_R^\dagger \boldsymbol{A} q_L + q_L^\dagger \boldsymbol{A}^\dagger q_R \,, \tag{28}$$

where the trace in (28) is over $\boldsymbol{x}$ and n. The partition function associated to (28) is simply

$$Z[T,\mu] = \langle \det{}_{2,\boldsymbol{x},n}\, \boldsymbol{Q} \rangle \,, \tag{29}$$

where the averaging is meant to be

$$\langle \ldots \rangle = \int d\boldsymbol{A} \ldots \mathrm{e}^{-N\Sigma \mathrm{Tr}_{\boldsymbol{x},n}(\boldsymbol{A}\boldsymbol{A}^\dagger)} \tag{30}$$

with the medium Dirac operator in a random background,

$$\boldsymbol{Q} = \begin{pmatrix} im & \boldsymbol{\Omega} + i\mu \\ \boldsymbol{\Omega} + i\mu & im \end{pmatrix} + \begin{pmatrix} 0 & \boldsymbol{A} \\ \boldsymbol{A}^\dagger & 0 \end{pmatrix} \equiv \boldsymbol{D} + \boldsymbol{R}. \tag{31}$$

The determinant in (29) is over chirality (2), space ($\boldsymbol{x}$), and frequency space (n). This is an example of a chiral random matrix model. When restricted to $n = 0$ with $\omega_0 = 0$ and $\mu = 0$, this is just the chiral random matrix discussed in [16] for one flavor.

With the transcription (29-31) the translation of the bulk arguments whether in vacuum (ground state) or matter (thermodynamics) can be made using the resolvent (one-point function) and its moments (multiple-point functions). Specifically, let

$$\boldsymbol{G}(z) = \frac{1}{N}\left\langle \mathrm{Tr}(z - \boldsymbol{Q})^{-1} \right\rangle \tag{32}$$

for the simple case $\boldsymbol{Q} = \boldsymbol{R}$ (purely random), where the averaging is carried over the Gaussian ensemble (30). Using the methods discussed in [17], the answer is found to be

$$\boldsymbol{G}(z) = \tfrac{1}{2}(z - \sqrt{z^2 - 4})\,. \tag{33}$$

The Dirac spectral density follows from

$$\nu(\lambda) = -\frac{1}{\pi}\lim_{\epsilon\to\infty} \boldsymbol{G}(z)|_{z=\lambda+i\epsilon} = \frac{1}{N}\left\langle \delta(\lambda - \boldsymbol{Q}) \right\rangle, \tag{34}$$

where we have used (24) and definition of average spectral density (last line). Hence

$$\nu(\lambda) = \frac{1}{2\pi}\sqrt{4 - \lambda^2} \tag{35}$$

in agreement with the numerical calculation using a set of 200 100×100 matrices with matrix elements randomly drawn from a Gaussian distribution, as shown in Fig. 2. At $\lambda = 0$, the spectral density $\nu(0) \neq 0$, and chiral symmetry is spontaneously broken.

In the presence of a deterministic part $\boldsymbol{D}$ (mass, temperature, chemical potential, θ angle, twist, *etc*) the Dirac spectrum is modified. Since the scale in the purely random case is of order one (Wigner semi-circle) a structural change in the Dirac spectrum (phase transition) is usually expected when the deterministic part becomes large. Such is the fate of the chiral phase transition in the random matrix analog of the two-level NJL model. This point can be made more quantitative, by considering how the random

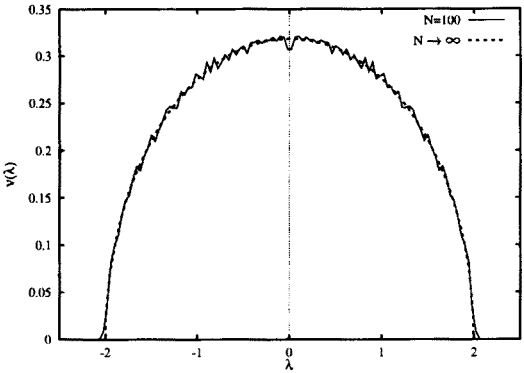

Fig. 2. Mean spectral distribution (dashed line) versus random drawings (solid line) — see text.

spectrum changes under the addition of the deterministic part. In the case of the pure random Gaussian plus deterministic this problem was solved years ago by Pastur [18]. In the case of non-Gaussian ensembles (not discussed here) more sophisticated methods are needed (R-transformation or, equivalently, Blue's function methods [19]).

Pastur equation states that

$$\boldsymbol{G}(z) = \boldsymbol{G}_D(z - \boldsymbol{G}(z))\,, \tag{36}$$

where $\boldsymbol{G}(z)$ is the Green's function for the random plus deterministic system and $\boldsymbol{G}_D$ is the Green function for the deterministic system only. For the case $\omega_0 = -\omega_{-1} = \pi T$, $\mu = 0$ and $m = 0$ the deterministic Green's function $\boldsymbol{G}_D$ corresponding to the deterministic part of (31), is by definition

$$\boldsymbol{G}_D(z) = \tfrac{1}{2}\left(\frac{1}{z - \pi T} + \frac{1}{z + \pi T}\right) \tag{37}$$

since the spectral function is $\nu_D(\lambda) = {}^1\!/_2(\delta(\lambda - \pi T) + \delta(\lambda + \pi T))$. Therefore

$$\boldsymbol{G}(z) = \tfrac{1}{2}\left(\frac{1}{z - \pi T - \boldsymbol{G}(z)} + \frac{1}{z + \pi T - \boldsymbol{G}(z)}\right). \tag{38}$$

This particular cubic equation was first obtained by Brézin, Hikami and Zee [20] in a general context, and used by others [21–25]. The imaginary part of the normalizable solution to this cubic equation gives the spectral distribution shown in Fig. 3.

For zero temperature we recover the semicircle shown at Fig. 2. For finite T the levels start to repel each other, building a dip around the origin. The thermal localization starts to show up, weakening the overall randomness

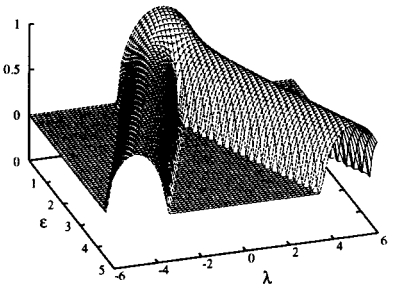

Fig. 3. Spectral distribution (C class) as a function of λ and $\epsilon = \pi T$

at zero temperature. For $T_c = 1/\pi$ (in units $\Sigma = 1$) the average spectral density reaches zero, thereby restoring chiral symmetry by the Banks-Casher formula. Further increase in the temperature results in splitting the spectra into two disconnected arcs. We call the phase transition $P_1 \to P_2$ type. The phase P_2 corresponds to a chirally symmetric phase. Although the present description of the phase transition in terms of the Dirac spectrum sounds a bit exotic, we recall from our thermodynamical description of the two-level NJL model that it has a direct correspondence with the conventional wisdom. In particular, the thermal transition described here is mean-field in character. Mean-field exponents control the behavior of the spectral density **near** the edge of the spectrum.

5. Cardano, Ferrari and Quinto classes

It is clear that the character of the Dirac spectrum near a phase transition depends on the number of competing scales carried in the deterministic part. In the large N limit, a simple classification can be reached from Pastur's equation (provided that the transition is not upset by fluctuations). Generically:

- Quadratic equation (Quadratic (K) class)
  In this case (pure random) Pastur equation reads
  $$\boldsymbol{G}^2(z) - z\boldsymbol{G}(z) + 1 = 0\,. \tag{39}$$
  The normalizable solution is just (33). The spectral density is a semi-circular and chiral symmetry is always broken.
- Cubic equation (Cardano (C) class)
  Pastur equation (38) reads
  $$\boldsymbol{G}^3(z) - 2z\boldsymbol{G}^2(z) + (z^2 - \epsilon^2 + 1)\boldsymbol{G}(z) - z = 0\,. \tag{40}$$

The normalizable solution is shown in Fig. 3. A phase transition sets in at $\epsilon = 1$. Equation (40) has various realizations:
1. Identifying ϵ with πT yields a model for the chiral phase transition [21].
2. Identifying ϵ with $\pi T - P$ (P is the Z_3 phase) probes in addition triality [22].
3. Identifying ϵ with m models lattice Wilson spectra [24].
4. Identifying ϵ with $\sqrt{m^2 + \pi^2 T^2}$ models lattice Kogut-Susskind spectra [23].
6. Identifying ϵ with $\pm 1/2$ models e^- scattering in quantum Hall liquids [19].

- Quartic equation (Ferrari (F) class)
1. An example is the two-random matrix model [26] as motivated by the two-component instanton model [27]. Pastur's equation in this case reads [25]

$$\boldsymbol{G}(z) = \alpha \frac{1}{z - \boldsymbol{G}(z)} + (1 - \alpha) \frac{z - \boldsymbol{G}(z)}{(z - \boldsymbol{G}(z))^2 - d^2}, \tag{41}$$

where $(1 - \alpha)$ is the percentage of molecules in the instanton vacuum and d is a measure of the quark-hopping strength between an instanton and an antiinstanton. Fig. 4 shows a typical behavior for the spectral density. The figure on the left displays a cohabitation phase between instantons and instanton-molecules. The figure in the middle shows the point when the molecules compete with the instantons (critical point). The figure on the right corresponds to the case where the molecules are not important. All critical exponents can be assessed analytically.

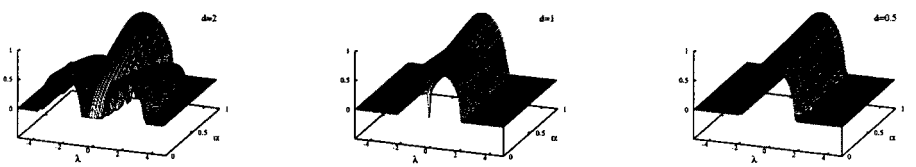

Fig. 4. Spectral distribution (F class) as a function of λ and $\epsilon = \alpha$ (concentration of molecules)

2. Another example of the F class is the random walk of a nonrelativistic particle of spin 0 or 1/2 in D-dimensions [28].
In general, the F classification allows for three phases, P_1, P_2, P_3.

- Fifth order equation (Quinto[2] (Q) class)
  A nontrivial example of this class is a model with two lowest pairs of Matsubara frequencies mixed coherently by the interaction [29]. Pastur equation reads in this case:

$$G^5 + a_4 G^4 + a_3 G^3 + a_2 G^2 + a_1 G + a_0 = 0 \tag{42}$$

with the coefficients

$$\begin{aligned} a_4 &= -4z\,, \\ a_3 &= 1 - (M_0^2 + M_1^2) + 6z^2\,, \\ a_2 &= -4z^3 - 3z + 2z(M_0^2 + M_1^2)\,, \\ a_1 &= \alpha(M_0^2 - M_1^2) - M_0^2(1 - M_1^2) + z^2\left[3 - (M_0^2 + M_1^2)\right] + z^4\,, \\ a_0 &= z\left[M_0^2 - \alpha(M_0^2 - M_1^2) - z^2\right]\,, \end{aligned}$$

where $M_0^2 = m^2 + \pi^2 T^2$, $M_1^2 = m^2 + 9\pi^2 T^2$. The Quinto class allows for a rich phase structure, with in general four possible phases P_1, P_2, P_3, P_4 defined by the number of disconnected arcs providing the support for the eigenvalue distribution. Fig. 5 (left) shows the distribution of eigenvalues as a function of temperature for the case of a single light flavor.

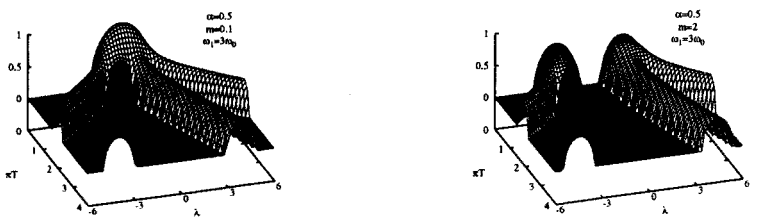

Fig. 5. Spectral distribution (Q class) as a function of λ and ϵ for two pairs of Matsubara modes

At zero temperature, the spectral function is peaked around zero, providing a non-zero condensate. The distribution of eigenvalues is given by Wigner's semicircle, the system is in the P_1 phase. As the temperature is increased, two effects happen. The rising temperature destroys the disorder, diminishing the value of the spectral function

[2] We use for short the name Quinto for the class of solutions of this equation, as a tribute to XVI century Italian mathematicians (Tartaglia, Cardano, Ferrari, Bombelli and others) working on the solutions to cubic and quartic equations.

at zero and leading finally to the restoration of the chiral symmetry ($\nu(0) = 0$). Simultaneously, the rising temperature starts splitting the Matsubara frequencies. Therefore the phase structure diagrams are: $P_1 \to P_2 \to P_4$ or $P_1 \to P_3 \to P_4$ or $P_1 \to P_4$, depending if the restoration of chiral symmetry precedes, follows or parallels the splitting of the frequencies, respectively. Fig. 5 (right) shows the distribution for the case of a single heavy (above critical value of mass) flavor. The disorder is always destroyed, independently of the temperature which can only split the Matsubara frequencies. The phase structure in this case is always $P_2 \to P_4$.

Since the general solutions of the fifth order algebraic equation do not exist in analytical form, the results shown in Figs 5 were obtained numerically. The four unphysical remaining roots of the equation are ruled out by the failure to reproduce required spectral properties (normalizability and positivity), so the displayed solutions are unique. All critical exponents are mean-field, as shown in Section 2.

The present arguments clearly generalize to higher polynomial equations showing both the richness and complexity of a phase transition when discussed using the Dirac spectrum. Higher polynomial equations are only tractable numerically as we have shown for the case of the Quinto class.

6. Finite temperature lattice results

Recent lattice simulations by the Columbia group [30] using staggered fermions have unraveled interesting aspects of the Dirac spectrum of two-flavor QCD in the semi-quenched approximation on a $16^3 \times 4$ and $32^3 \times 4$ lattices. If we were to denote by ζ the valence quarks with mass m_ζ, then the valence quark condensate [30]

$$\langle \bar{\zeta}\zeta \rangle (m_\zeta) = 2m_\zeta \int_0^\infty d\lambda \, \frac{\nu(\lambda)}{\lambda^2 + m_\zeta^2}, \tag{43}$$

where $\nu(\lambda)$ is the Dirac eigenvalue distributions associated to $i\not{D}$ for two-flavor and massive QCD. The third flavor ζ is not included while averaging over the sea fermions. The dependence on the sea mass m_s (not to be confused with strangeness) and the number of flavors in $\nu(\lambda)$, stem from the random averaging over the gauge configurations in the presence of the two-flavor fermion determinant [30]. For two degenerate flavors with $m_s a = 0.01$, the behavior of (43) versus m_ζ on a $16^3 \times 4$ lattice is shown in Fig. 6 (left), for eight temperatures $\beta = 6/g^2$ around the critical temperature $\beta_c = 5.275$. The transition in this case is believed to be second order, with a critical

temperature $T_c = 1/4a \sim 150$ MeV [31]. In physical units, the lattice spacing at the critical temperature is $a \sim .33$ fm, and the sea quark mass is $m_s = 6$ MeV.

In Fig. 6 (right), we show the behavior of the valence quark condensate for a sea quark mass of 0.1, and various β (temperature) values as obtained from the Cardano solution for Pastur equation with $\epsilon = \sqrt{m_s^2 + \pi^2 T^2}$. The plotted curves were obtained analytically. In physical units the sea quark mass equals 10 MeV. We have identified β with T,

$$\pi(T - T_c) = (\beta - \beta_c) \tag{44}$$

with the critical temperature T_c in the chiral random matrix model and $\beta_c = 5.275$ as suggested by the lattice calculations [30]. The transition in the chiral random matrix model is mean-field in character (large N). For a small mass $m_s = 0.1$ (10 MeV) the random matrix model seems to follow qualitatively well the lattice results for $m_s a = 0.01$ (6 MeV), except for $m_\zeta \leq 10^{-5}$, where the spectrum becomes sensitive to the finite size of the lattice, as illustrated by the bending of the upper curves. Finite size effects set in when the pion Compton wavelength becomes comparable to the lattice size. Using the PCAC relation this implies that $m_\zeta \langle \bar{\zeta}\zeta \rangle \geq 1/N_c V_4$. For $V_4 = 4 \times 16^3$, this puts a lower bound on the valence mass $m_\zeta \geq 10^{-4}$, which is about consistent with the lattice results.

The quantitative agreement between the lattice simulations and the two-level NJL model or the chiral random matrix model, is surprising to say the least. Does it confirm the assumption made above about scale separations? Does it imply that the temperature is indeed high enough to motivate a constituent quark description with few Matsubara modes? Is the chiral restoration insensitive to the issue of confinement? These are all important questions that require further analysis. In this sense, it would be helpful if the lattice results were also available after **cooling**.

Having said this, we note that the reading of the critical temperature β_c depends sensitively on the value of the sea quark mass. In matrix models, for $m_s = 0$, the critical temperature is $\beta = 5.275$, whereas for $m_s = 0.1$, the critical value is $\beta = 5.27$ (the fourth line from the top on right figure). In the random matrix model (Cardano solution), the shift in the critical temperature on the sea quark mass comes simply from $\Delta\beta_c = \sqrt{1 - m_s^2} - 1$. This behavior agrees with lattice data. The critical line has mean-field exponent $\delta = 3$ (mean-field): for $\beta = 5.275$, $\langle \bar{\zeta}\zeta \rangle \sim m_\zeta^{0.33}$. This value is to be contrasted with the one quoted by Chandrasekharan and Christ [30], namely $\langle \bar{\zeta}\zeta \rangle \sim m_\zeta^{0.6}$ for $\beta = 5.275$. We recall that a two-flavor simulation of QCD using finite-temperature cumulants yields $1/\delta$ in the range 0.21-0.26 [32], hence closer to the mean-field result. The value for $1/\delta$ cited by [32] is very close to suspected from universality values 0.206(9) (for $O(4)$

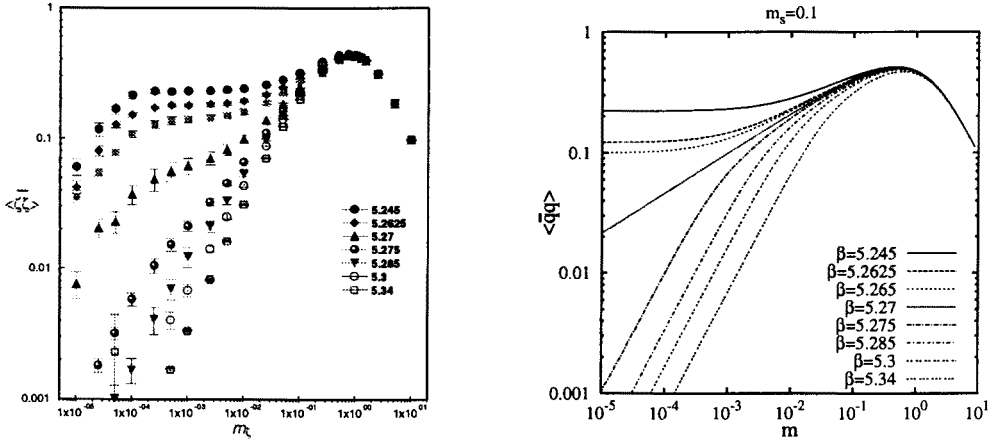

Fig. 6. Semi-quenched condensate (43) versus the valence quark mass m_ζ for two-flavor QCD. Left are the lattice results from [30]. Right are the Cardano results with $m_s = 0.1$.

three dimensional Heisenberg model) and 0.2072(3) (for $O(2)$ model). Other critical exponents calculated by [32] are however in disagreement with both universality classes. So the value of δ for QCD and its relation to mean-field is still a debated issue.

The other critical exponent from the Columbia data, $\langle\bar{\zeta}\zeta\rangle \sim m_\zeta^{0.98}$ for $\beta = 5.34$, agrees with the mean-field value $\langle\bar{\zeta}\zeta\rangle \sim m_\zeta^{1.00}$. The closeness of the last exponent to the random matrix result, suggests perhaps an underestimation of the critical exponent $1/\delta = 0.6$ [30] in comparison with the mean-field one $1/\delta = 0.333$, possibly due to the large finite sizes effects mentioned above as visible in Fig. 6 (dropping plateau's for small masses). Other quantitative features, like the U(1) jump, show also some similarity to the random matrix model results:

The present analysis involves one pair of Matsubara frequencies (Cardano Class). While this is expected to be dominant at high temperature, the comparison with the Columbia data at the critical temperature, requires that the role of more Matsubara modes be investigated. The case of two Matsubara modes can be studied using similar techniques [29]. In this case, we note that the character of Pastur's equation depends on the way the Matsubara frequencies are coupled. In the free case, the resulting equation is a superposition of two Cardano's, each for each Matsubara frequency. In the case where they are mixed, they result into a Quinto equation. Both scenarios are distinguishable by the ratios of their critical parameters. Indeed,

in the Quinto class the critical temperature is expected to set in at

$$4\pi^2\Sigma_Q^2 T_c^2 = \tfrac{10}{9}(1 - 2\Sigma_Q^2 m_s^2) + \sqrt{\tfrac{100}{81}(1 - 2\Sigma_Q^2 m_s^2)^2 - \tfrac{16}{9}\Sigma_Q^2 m_s^2(\Sigma_Q^2 m_s^2 - 1)}\,. \quad (45)$$

For zero quark mass (45) gives $\pi^2 T^2 = 5/9\,\Sigma_Q^2$, where Σ_Q is the spread in the Gaussian ensemble. The critical mass (denoted by star), at which the condensate vanishes (zero temperature) is $m_s^* = 1/\Sigma_Q^2$. A comparison of these results (mixing) to the ones following from the superposition of two Cardano's (non-mixing) follows from the identification $2\Sigma_Q^2 = \Sigma_C^2 = 1$. For the Cardano class

$$\pi^2 T_c^2 = 1 - m_s^2 \quad (46)$$

so that $T_c = 1/\pi$ in the massless case, and $m_s = 1$ in the zero temperature case. The ratio of the critical parameters in the two scenarios is

$$\frac{\pi T_c}{m_s^*} = \begin{cases} 1 & \text{for Cardano class} \\ \sqrt{\frac{5}{9}} & \text{for Quinto class} \end{cases} . \quad (47)$$

7. Finite density lattice results

From the two-level NJL model we expect a chiral restoring transition to take place when the chemical potential reaches the value of the constituent quark mass m_Q (zero baryon density), in agreement with the mean-field analysis. This transition is also confirmed in a large N analysis of the singularities associated to Pastur's equation (C class) with $\epsilon = i\mu$. Indeed an elementary study of the singularities, show a first order transition at $\mu\Sigma = \sqrt{1/8} = m_Q\Sigma$ [10] using the free energy in the fermionic variables [3]

Quenched QCD lattice simulations suggest a first order transition at $\mu = 0$ in the chiral limit [34]. Is this a way to **infirm** the above models? Not really, since a chiral transition at $\mu = 0$ is unphysical in the first place. So what is going on? To understand the subtleties behind the quenched lattice simulations, and also the present large N arguments, let us consider the **unquenched** generating function with $2N_f$ quarks and finite μ,

$$\boldsymbol{Z}(z, 2N_f, \mu) = \langle \det{}^{2N_f}(z - \boldsymbol{Q}) \rangle \quad (48)$$

[3] In Ref. [33] this transition was deemed second order at $\mu^2 = 0.278$ using the free energy in the bosonic variables. The discrepancy is, however, irrelevant since both mean-field analyses are upset by fluctuations.

with $V_{2N_f} = -\log Z/2N_f$ playing the role of a complex potential. Since $(z - \boldsymbol{Q})$ is non-hermitean for finite chemical potential, we can split it into a phase and a modulus through

$$(z - \boldsymbol{Q})^2 = |z - \boldsymbol{Q}|^2 \times (\frac{z - \boldsymbol{Q}}{\bar{z} - \boldsymbol{Q}^\dagger}) . \tag{49}$$

In terms of (48)–(49), the symmetric spectral density in the quenched approximation reads for finite N and N_f (chiral limit)

$$\nu(z, \bar{z}) = -\frac{1}{2\pi N} \left(\partial_{\bar{z}} \partial_z V_{2N_f} + \partial_z \partial_{\bar{z}} V_{2N_f} \right) . \tag{50}$$

The contribution of the modulus is

$$\nu_1(z, \bar{z}) = \nu(z) - \frac{N_f}{2\pi N} \langle \mathrm{Tr}(z - \boldsymbol{Q})^{-1} \mathrm{Tr}(\bar{z} - \boldsymbol{Q}^\dagger)^{-1} \rangle_c + \dots , \tag{51}$$

while the contribution of the phase is

$$\nu_2(z, \bar{z}) = \frac{N_f}{2\pi N} \langle \mathrm{Tr}(z - \boldsymbol{Q})^{-1} \mathrm{Tr}(\bar{z} - \boldsymbol{Q}^\dagger)^{-1} \rangle_c + \dots . \tag{52}$$

Here the subscript c is for connected. The density $\nu(z, \bar{z})$ is the sum of (51) and (52) modulo an extra contributions from the crossed terms. The connected two-point function

$$N^2 \boldsymbol{C}(z, \bar{z}) = \langle \mathrm{Tr}(z - \boldsymbol{Q})^{-1} \mathrm{Tr}(\bar{z} - \boldsymbol{Q}^\dagger)^{-1} \rangle_c \tag{53}$$

appears with opposite signs in the modulus and the phase, and cancels in the sum.

For finite N and $N_f \to 0$ (quenched approximation), the symmetric density reduces to $\nu(z)$. In the large N limit, the latter follows from the discontinuities of the one-point Green's function in the mean-field approximation. For $\mu^2 \leq 1/8$ chiral symmetry was found to be broken. The mismatch of this result with the quenched lattice calculations, suggests that the large N limit does not necessarily commute with the quenched limit $N_f \to 0$. This important point was first made by Stephanov[33] using mean-field arguments, in agreement with earlier results [35]. In our case, it follows from the singularities of (53). Using the random matrix model, (53) reads [36, 37]

$$N^2 \boldsymbol{C}(z, \bar{z}) = -\tfrac{1}{4} \partial_z \partial_{\bar{z}} \mathrm{Log}\{[(\boldsymbol{H} - \mu^2)^2 - |z - \boldsymbol{G}|^4]/\boldsymbol{H}^2\} , \tag{54}$$

where $\boldsymbol{H} = |z - \boldsymbol{G}|^2/|\boldsymbol{G}|^2$ and $\boldsymbol{G}(z)$ is a solution to Pastur's equation (40) with $\epsilon = i\mu$. From (54) we observe that the two-point correlation function

diverges in the eigenvalue-plane in the domain prescribed by the zero of the logarithm,

$$|z - \boldsymbol{G}(z)|^2(1 - |\boldsymbol{G}(z)|^2) - \mu^2|\boldsymbol{G}(z)|^2 = 0\,. \tag{55}$$

Fig. 7 shows the envelope in dashed line for which the condition (55) is met in the $w = iz$ plane, for several values of the chemical potential μ. The dots show the simulated results for an ensemble of 200 complex matrices 100×100. The solid bars are the mean-field solution following from Pastur equation. A structural change takes place at $\mu^2 = 1$ which is to be compared with $\mu^2 = 1/8$ in the naive quenched approximation. The onset of the mean-field transition is seen by an inward folding (vertical direction) in the dashed curve. At large μ^2 (essentially $\mu^2 \sim 8$), the envelope surrounds the cuts very closely. We have checked analytically that the general condition (55) is in agreement with the result of Ref. [33]. The universal form of the correlator (54) allows a generalization of the present results to finite mass and temperature, as well as non-Gaussian weights. Figs 8 and 9 display some sample analytical results compared to numerical simulations (dots) [37].

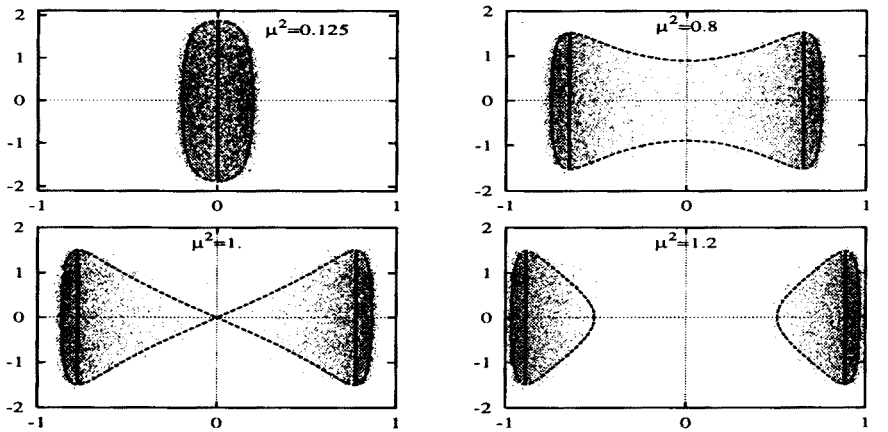

Fig. 7. Envelope (dashed lines) from Eq. (55) in the plane $w = iz$ while the cuts (solid lines) are from Pastur equation, for different μ. The dots are the results of a numerical calculation.

The above arguments show that the $1/N$ fluctuations upset the mean-field result on the envelope of Fig. 7 : there is a phase change. If we were to note that $\nu(z, \bar{z})$ is a measure of the quenched quark condensate $\langle q^\dagger q\rangle$ or its conjugate $\langle Q^\dagger Q\rangle$ as $z \to 0$, then

$$N^2\boldsymbol{C}(z, \bar{z}) = \langle q^\dagger q\; Q^\dagger Q\rangle_c\,. \tag{56}$$

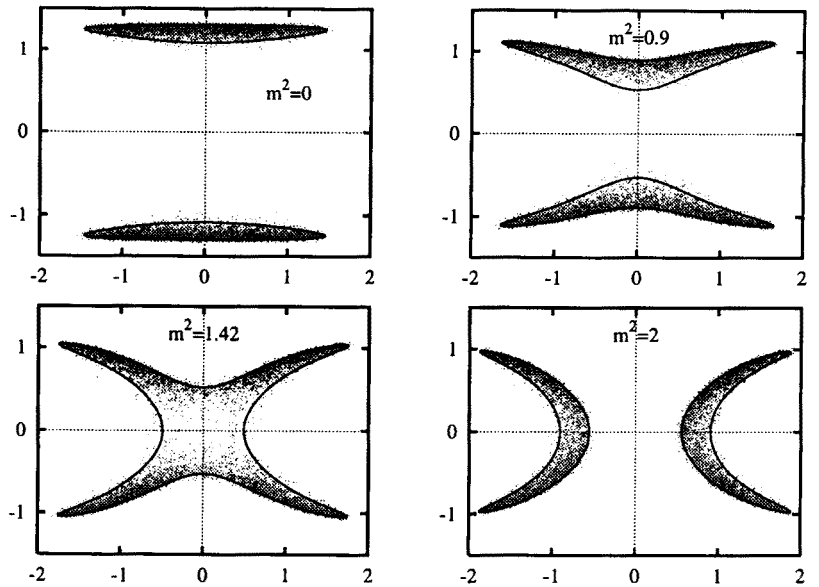

Fig. 8. Same as Fig. 7 but for $\mu^2 = 2$ and various masses in the z-plane.

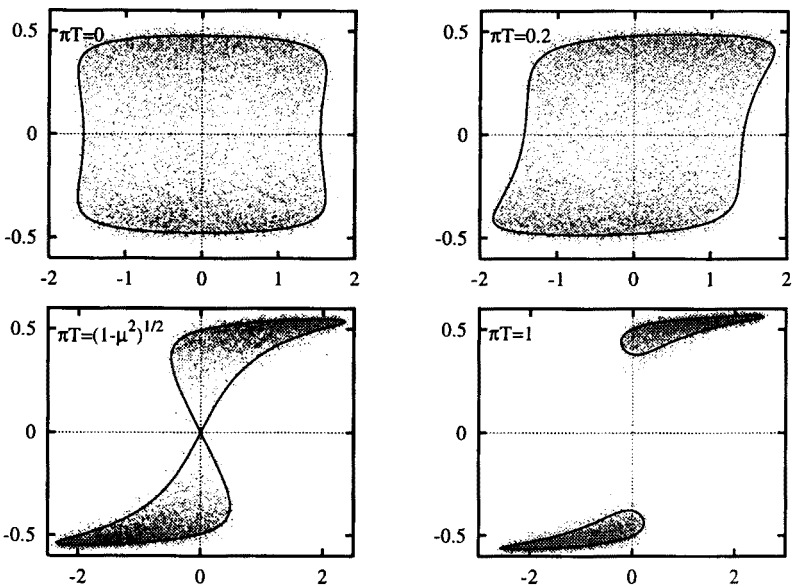

Fig. 9. Same as Fig. 7 but for $\mu^2 = 0.4$ and different temperatures in the z-plane.

In the usual vacuum with spontaneously broken chiral symmetry and $\mu = 0$, $\langle q^\dagger q \rangle$ and $\langle Q^\dagger Q \rangle$ are nonzero. Hence, the leading N contribution to (56) vanishes, and by the central limit theorem (56) is of order $\sqrt{N}$ or less. As a result, the contribution of the correlator is of order $N_f/\sqrt{N}$ or less. The expansion in N_f for the Green's function is asymptotic in the full z-plane minus the cut on the real axis, and the quenched limit commutes with the thermodynamical limit $N \to \infty$.

For small μ the fermion determinant develops a complex part. In the complex eigenvalue plane, (56) through (55) diverges when closing on the dashed curve of Fig. 7 from the outside. This is a signal that (56) is receiving increasingly large contributions from the mixed condensates $\langle q^\dagger Q \rangle$ and their conjugates $\langle Q^\dagger q \rangle$ (other "vacuum"). Hence (56) is qualitatively of order N in the domain encircled by the dashed curve in Fig. 6. As a result the correlation function contributes a term of order $N_f N^0$. The expansion in N_f for the Green's function is asymptotic in the z-plane minus the shaded domains encircled by the dashed curves in Fig. 6.

The conjugate quarks Q carry the same quantum numbers as the original quarks q except that they have **opposite** baryon number. By the Gell-Mann–Nishijima relation, they would carry fractional charges, and hence are just theoretical constructs. So should we take seriously the above results? In a way yes, since they seem to tell us that **any** finite μ causes large fluctuations in the lattice and model Dirac spectra. So something ought to be wrong with the hadronic spectrum in both cases.

For two-color QCD, baryons are "Goldstone" modes. They carry the analog of the pion mass. Any finite chemical potential causes them to condense in the chiral limit, so it is logical that a chiral phase transition sets in at $\mu = 0$. But what about three-color QCD? Before we attempt to answer this question, we note that in the two-level NJL model described above, of which the chiral random matrix model is just a version, we have **omitted** from the above thermodynamical arguments the contribution of the multiquark excitations. Since the model does not confine, they may contribute substantially to the pressure thereby explaining the failure of the large N argument with only the **naive** constituent quark spectrum. A simple analysis of the model of Section 2 shows that the scalar-isoscalar diquark is indeed massless! Hence, the low μ phase is dominated by diquarks **instead** of constituent quarks. The transition sets in at $\mu = 0$, in agreement with the above results [4]. We **note** that in conventional NJL models diquarks are in general massive [38], due to the internal kinetic energy of the two quarks, so the problem may not arise.

[4] Since the finite temperature arguments discussed above were carried from the high temperature side of the chiral phase transition, the contribution of the diquark-antidiquark modes is suppressed owing to entropy.

For the quenched lattice simulations, confinement is not really an issue, or is it? The fact that the quenched simulations show a similar behavior as a function of μ, suggests similar problems in the hadronic spectrum of quenched QCD. Indeed, it was pointed out by Kogut and his collaborators [39], that while confinement is a property of the ensemble average it is not of each sampled gauge configuration. Due to the periodic character of the lattice, the light quark configurations that wind several times around the lattice, are only suppressed in the large volume limit on the average. At finite chemical potential, an unbalance is triggered between the forward and backward going loops that may not necessarily balance in the large volume limit, as exemplified by the behavior of the "baryonic" pion correlation function. Although we do not know how these winding modes show up in a hadronic spectrum in Minkowski-space-time, we **suspect** that they may be close cousins of the multiquark states! Perhaps the only way to enforce confinement properly on the lattice at finite chemical potential is to resort to a canonical simulation instead of the grand-canonical one currently in use [39].

8. Random matrix models and QCD

The few examples presented above provide some interesting insights to complex lattice simulations in the region of the phase transition (finite temperature). They seem to embody also the same inherent subtleties observed on the lattice (finite chemical potential). So **why** if at all, a two-level NJL, model or chiral random matrix models bear at all on QCD, in the mean-field approximation?

The qualitative answer to this question in a way lies in the type of observables we have chosen to present and the intrinsic assumption we have made. Indeed, we have assumed that chiral symmetry is spontaneously broken from the start, by choosing the number of constant quark modes to be commensurate with the volume of the system. In such an ensemble, the fine details of the interaction between the constant quark states become irrelevant, provided that they obey the strictures of chiral symmetry. The distribution of these modes is controlled by the general lore of randomness and symmetry in the vacuum.

In QCD, these soft modes are likely to set in around instanton configurations or any of their topological relatives. Since cooling on the lattice has been shown to maintain the gross features of QCD in the infrared [40], it is not surprising that a simplified approach of the type we have discussed works for the bulk structure of the QCD Dirac spectrum. The

random matrix model can be seen as a schematic description of the quark zero modes in a random instanton vacuum. In fact it was originally concocted after that model.

In the presence of some external parameters, such as the mass, temperature or density, the dynamics of these constant modes follows the general competition between randomness and determinism : a give and take between delocalization (randomness) and localization (determinism). A phase transition takes place at the breaking point in the distribution of eigenvalues, under the **unspelled** assumption that the hard modes remain **decoupled**. This assumption is particularly important to check on the lattice by addressing the issue of the phase transition before and after cooling. The above analysis shows that the gross features of the phase transition are equally well addressed using the Dirac spectrum or conventional mean-field arguments, both of which seem to be consistent with the lattice simulations **quantitatively**. This point suggests that the chiral phase transition in QCD is largely mean-field in character, with a narrow Ginzburg window.

Clearly the schematic models discussed here have nothing to say on the detail distributions of quarks in hadrons, their space-time variation in color singlet configurations, nor they bear on the gluonic content of the vacuum and the behavior of the Polyakov line. Such questions involve detailed knowledge of the quark and gluon wave-functions, and pertain to the femtoworld of dynamical QCD. So under what **specific** assumptions in QCD could we get back a two-level NJL model? We can only guess. For instance, if the instanton model to the QCD vacuum could be made more quantitative by resolving the issue of the short range instanton-antiinstanton interaction and through lattice comparisons, then we may think of the present models as a schematic description of the zero-mode sector of semi-classical QCD in the large volume limit. More speculatively, we may also think of random matrix models as the embodiment of the master field in large N_c (number of colors) QCD [41]. Indeed, the set of master fields in QCD reduces to four space-time independent $N_c \times N_c$ matrices plus an external momentum [42]. In the presence of quarks, it may be enough to think of these fields as purely random.

9. Random matrix models and universality

Since chiral random matrix models are an efficient way to quantify the universal role of noise in spectra, we may finally ask which of the above results obey microscopic universality? The answer is none. Most of our discussion has focused on the bulk distribution of the spectrum, hence non-universal. Universality in the sense of Wigner and Dyson is realized in the form of spectral oscillations at the level of one-level spacing [16]. How it may

show up in physical observables is in so far unclear to us, especially in light of the differences between the oscillations and the fermion realizations on the lattice. Continuum, macroscopic QCD appears to be deaf to the universal noise of the microscopic limit. What about macroscopic universality in random matrix models? The level correlation discussed in (53)–(54) obeys macroscopic universality [43]. Independently of the measure used (provided that it is local), the form of the correlation depends only on the character of the random matrix model. We suspect that this macroscopic universality may be tied to some underlying Ward identities that are shared by macroscopic QCD in some limit.

10. Summary

Using a schematic version of the NJL model, we have discussed some elementary aspects of the thermodynamics and their relation to the chiral phase transition and universality (mean-field) arguments. We have shown how a chiral random matrix model follows from this schematic form of the NJL model, thereby translating the character of the phase transition to the Dirac spectrum. Some interesting comparisons to the bulk lattice simulations were made. As a truncated version of QCD to space-time independent quark modes, the model presented here has obvious shortcomings. This notwithstanding, since the model embodies symmetries, randomness and some basic scales, it can serve as a reference point for more serious approaches to the finite temperature/density phase transition in QCD. In particular, it can be used to sort out the issue of dynamics from that of symmetries and noise.

We thank Jurek Jurkiewicz for discussions and Gerry Brown for encouragements. M.A.N. would like to thank Profs. L. Jarczyk, A. Bałanda, R. Kulessa and Dr. A. Magiera and other organizers of MESON'96 for the invitation and the hospitality. This work was supported in part by the US DOE grant DE-FG-88ER40388, by the Polish Government Project (KBN) grants 2P03B19609 and 2P03B08308 and by the Hungarian Research Foundation OTKA.

REFERENCES

[1] R.D. Pisarski, *Phys. Lett.* **B100**, 155 (1982); A.I. Bochkarev, M.E. Shaposnikov, *Nucl. Phys.* **B268**, 220 (1986); G.E. Brown, M. Rho, *Phys. Rev. Lett.* **66**, 2720 (1991).

[2] K. Kanaya, *Nucl. Phys.* (Proc. Suppl.) **B47**, (1996).

[3] for a review, see *e.g.* E. V.Shuryak, *Rev. Mod. Phys.* **65**, 1 (1993); D. Diakonov, Chiral Symmetry Breaking by Instantons, eprint hep-ph/9602375.

[4] A.I. Bochkarev, M.E. Shaposhnikov, *Nucl. Phys.* **B268**, 220 (1986); T. Hatsuda, S.H. Lee, *Phys. Rev.* **C46**, 34 (1992); C.A. Dominguez, M. Loewe, J.C. Rojas, *Z. Phys.* **C59**, 63 (1993).

[5] for an introduction, see H. Leutwyler, Principles of Chiral Perturbation Theory (lectures given at "Hadrons 94", Gramado, RS, Brasil, Bern preprint BUTP-94/13.

[6] T. Hatsuda, T. Kunihiro, *Phys. Rev. Lett.* **55**, 158 (1985); V. Bernard, U.G. Meissner, I. Zahed, *Phys. Rev.* **D36**, 819 (1987); M. Lutz, S. Klimt, W. Weise, *Nucl. Phys.* **A542**, 521 (1992); G. Ripka, M. Jaminon, *Ann. Phys.* **218**, 51 (1992).

[7] G.E. Brown, M. Buballa, M. Rho, A Mean Field Theory of the Chiral Phase Transition", eprint nucl-th/9603016.

[8] J.J.M. Verbaarschot, in *Continuous Advances in QCD,* Ed. A.V. Smilga, World Scientific, Singapore 1994.

[9] for a broad overview see M.A. Nowak, M. Rho, I. Zahed, *Chiral Nuclear Dynamics*, World-Scientific, Singapore 1996, in print.

[10] R. A. Janik, M.A. Nowak, I. Zahed, Chiral Random Matrix Models: eprint hep-ph/9604253.

[11] J.I. Kapusta, *Finite-Temperature Field Theory*, Cambridge Univ. Press 1989.

[12] R. Pisarski, F. Wilczek, *Phys. Rev.* **D29**, 338 (1984).

[13] T. Banks, A. Casher, *Nucl. Phys.* **B169**, 103 (1986).

[14] H. Neuberger, *Phys. Lett.* **B112**, 341 (1982); A. Casher, H. Neuberger, *Phys. Lett.* **B139**, 67 (1984).

[15] T. Kalkreuter, Numerical analysis of the spectrum of the Dirac operator in four dimensional SU(2) gauge fields, eprint hep-lat/9511009.

[16] E.V. Shuryak, J.J.M. Verbaarschot, *Nucl. Phys.* **A560**, 306 (1993); J.J.M. Verbaarschot, I. Zahed, *Phys. Rev. Lett.* **70**, 3852 (1993). J.J.M. Verbaarschot, *Nucl. Phys.* **B427**, 534 (1994).

[17] See *e.g.*, C.E. Porter, *Statistical Theories of Spectra: Fluctuations*, Academic Press, New York 1965; M.L. Mehta, *Random Matrices*, Academic Press, New York 1991.

[18] L.A. Pastur, *Theor. Mat. Phys.* (USSR) **10**, 67 (1972).

[19] for an excellent introduction, see A. Zee, Law of addition in random matrix theory, eprint cond-mat/9602146.

[20] E. Brézin, S. Hikami, A. Zee, Universal correlations for deterministic plus random Hamiltonians, eprint hep-th/9412230.

[21] A.D. Jackson, J.J.M. Verbaarschot, A random matrix model for chiral symmetry breaking, SUNY-NTG-95/26, eprint hep-ph/9509324.
[22] M. Stephanov, Chiral symmetry at finite temperature, the phase of the polyakov loop and the spectrum of the Dirac operator, eprint hep-lat/9601001.
[23] M.A. Nowak, G. Papp, I. Zahed, Lattice QCD spectra at finite temperature: a random matrix approach, eprint hep-ph/9604235.
[24] J. Jurkiewicz, M.A. Nowak, I. Zahed, Dirac spectrum in QCD and quark masses, e-print hep-ph/9603308.
[25] M.A. Nowak, G. Papp, I. Zahed, QCD-inspired spectra from Blue's functions, eprint hep-ph/9603348.
[26] T. Wettig, A. Schäfer,and H.A. Weidenmúller, The chiral phase transition in a random matrix model with molecular correlations, eprint hep-ph/9510258.
[27] E.M. Ilgenfritz, E.V. Shuryak, *Nucl. Phys.* **B319**, 511 (1989).
[28] M. Engelhardt, Nonrelativistic Particle in Free Random Gauge Background, eprint hep-th/9604012.
[29] R.A. Janik, J. Jurkiewicz, M.A. Nowak, G. Papp, I. Zahed, *Phys. Rep.* (in preparation).
[30] S. Chandrasekharan, N. Christ, Dirac Spectrum, Axial Anomaly and the QCD Chiral Phase Transition, eprint hep-lat/9509095.
[31] C. DeTar, *Nucl. Phys.* (Proc. Suppl.) **B42**, 73 (1995).
[32] F. Karsch, E. Laermann, Susceptibilities, the specific heat and a cumulant in two-flavor QCD, BI-TP 94-29.
[33] M. Stephanov, *Phys. Rev. Lett.* **76**, 137 (1996).
[34] I. Barbour *et al.*, *Nucl. Phys.* **B275**, 296 (1986); E. Dagotto, A. Moro, U. Wolff, *Phys. Rev. Lett.* **57**, 1292 (1986); C.T.H. Davies, E.G. Klepfish, *Phys. Lett.* **B256**, 68 (1991); J.B. Kogut, M.P. Lombardo, D.K. Sinclair, *Phys. Rev.* **D51**, 1282 (1995).
[35] P.E. Gibbs, *Phys. Lett.* **B182**, 369 (1986); A. Gocksch, *Phys. Rev. Lett.* **61**, 2054 (1988).
[36] R.A. Janik, M.A. Nowak, G. Papp, I. Zahed, Brezin-Zee Universality: Why Quenched QCD in Matter is Subtle?, eprint hep-ph/9606329.
[37] R.A. Janik, M.A. Nowak, G. Papp, I. Zahed, to be published.
[38] R.G. Betman, L. Laperashvili, *Sov. J. Nucl. Phys.* **41**, 295 (1985); R.T. Cahill, C.D. Roberts, J. Praschifka, *Phys. Rev.* **D36**, 2804 (1987); V. Thorsson, I. Zahed, *Phys. Rev.* **D41**, 3442 (1990); D. Kahana, U. Vogl, *Phys. Lett.* **B244**, 10 (1990).
[39] J.B. Kogut, M.P. Lombardo, D.K. Sinclair, *Phys. Rev.* **D51**, 1282 (1995); *Nucl. Phys.* (Proc. Suppl.) **B42**, 514 (1995).
[40] M.-C. Chu, J. M. Grandy, S. Huang, J.W. Negele, *Phys. Rev. Lett.* **70**, 225 (1993); *Phys. Rev.* **D48**, 3340 (1993).
[41] E. Witten, in *Recent Developments in Gauge Theories*, ed. G.'t Hooft *et al.*, Plenum NY 1980.
[42] D.J. Gross, R. Gopakumar, *Nucl. Phys.* **B451**, 379 (1995).
[43] J. Ambjørn, J. Jurkiewicz, Y. Makeenko, *Phys. Lett.* **B251**, 517 (1990); E. Brezin, A. Zee, *Nucl. Phys.* **B402**, 613 (1993).